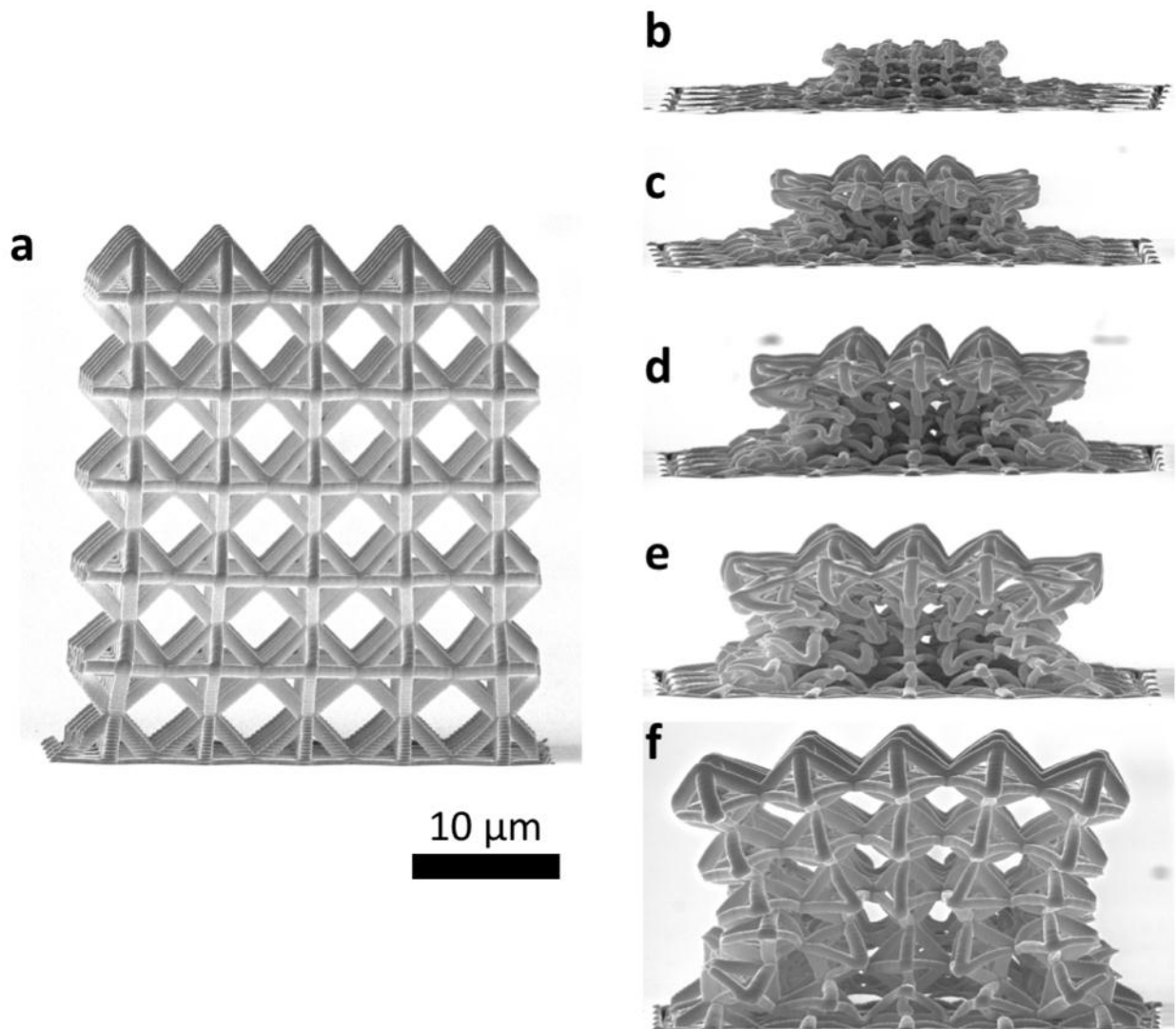


## Supporting Information

### Contraction of Thinner-walled Nanolattices

As mentioned in section 2.2, irradiation caused dramatic collapse in the nanolattice structure for all but the thickest-walled nanolattices, those fabricated with the longest sputter deposition time of 240 minutes, which corresponds to a median wall thickness of  $\sim 88$  nm. All the mechanical analysis was conducted on these thickest walled nanolattices but it is still interesting to view the contraction of the thinner-walled nanolattices. Figure A.1 (b-f) displays the SEM images of the thinner-walled nanolattices ( $\sim 57$  nm median wall thickness and less) following irradiation. For comparison, Figure A.1 (a) contains an image of a typical nanolattice before irradiation to illustrate the dramatic changes in nanolattice structure that occurs upon irradiation. The contraction is most severe in the thinnest walled nanolattices (wall thickness  $\sim 10$  nm) pictured in Figure A.1 (b) and becomes less severe as the nanolattice wall thickness is increased from (b) to (f). As all of the thinner-walled nanolattices pictured in Figure A.1 (b-f) underwent such significant contraction, they were not further characterized or compressed.

The presence of contraction in the structure of the nanolattices upon irradiation renders any changes in mechanical response a convolution of the atomic-level changes in the constituent metallic glass with these structural changes in the nanolattices. The thinner-walled nanolattices, pictured in Figure A.1, underwent such significant contraction upon irradiation that we chose not to conduct compression experiments on those nanolattices, as the mechanical response would likely be dominated by the contraction of the structure. Compression experiments were only performed on the thickest-walled nanolattices, pictured in Figure 2, which exhibited the smallest structural change upon irradiation. Although the overall structure of these thicker-walled nanolattices does exhibit some contraction upon irradiation, as visualized in Figure 2 (d), the wall thickness and inner beam dimensions are largely unchanged upon irradiation, as indicated by Tables 1 and 2.



**Figure A.1. Contraction of thinner-walled nanolattices upon irradiation.** SEM images of nanolattices were taken with a  $\sim 87^\circ$  stage tilt and the  $10\ \mu\text{m}$  scale bar applies to all images. (a) Typical nanolattice with  $\sim 38\ \text{nm}$  median wall thickness prior to irradiation. (b-f) Nanolattices after exposure to irradiation have undergone various degrees of contraction. The original wall thicknesses of the nanolattices prior to irradiation were (b)  $10\ \text{nm}$ , (c)  $20\ \text{nm}$ , (d)  $30\ \text{nm}$ , (e)  $38\ \text{nm}$ , (f)  $57\ \text{nm}$ . The contraction becomes less severe as the wall thickness is increased from (b) to (f).

### Details of nanolattice geometry measurements and relative density calculation

To obtain the wall thickness measurements analysis on the nanolattices, a series of cross-sectional cuts were performed as discussed in section 2.3. For each cross-sectional cut, we obtained  $\sim 20$  wall thickness measurements of wall thickness. With these six cross-sectional cuts and 20 measurements for each cut, there was a representative sample of  $\sim 120$  wall thickness measurements spanning the entire nanolattice from which the median and average wall thicknesses were determined. Similarly, the vertical (major) axes

and horizontal (minor) axes of the slightly elliptical shaped beams making up the nanolattices were also measured for each of the six cross-sectional cuts. From each cross-sectional cut,  $\sim 5$  measurements of each beam axis were obtained on beams favorably oriented with the  $\sim 52^\circ$  tilt of the SEM stage utilized for FIB operation. With these six cross-sectional cuts and 5 measurements from each cut, there was a representative sample of  $\sim 30$  beam axis measurements on each of the vertical and horizontal beam axes spanning the entire nanolattice from which the average beam dimensions were determined. This identical measurement procedure was conducted on nanolattices in the as-fabricated and irradiated states to facilitate direct comparison.

To obtain the beam measurements displayed in Table 2, both the vertical (major) beam axis and the horizontal (minor) beam axis were measured as the beams were not perfectly circular. As can be observed in Table 2, the original slightly elliptical shape of the beams became more pronounced upon irradiation as the vertical (major) beam axis increased from 803 nm to 867 nm while the horizontal (minor) beam axis decreased from 751 nm to 713 nm. Consistent with the general distortion and shape changes upon irradiation observed in Figure 2, the standard deviations in the measured beam dimensions increase by roughly a factor of two upon irradiation; the standard deviation in the vertical beam axes increase from 66.6 nm to 125 nm upon irradiation, and the standard deviation in the horizontal beam axes increase from 42.7 nm to 95.3 nm upon irradiation. However, the simultaneous increase in the vertical beam axis with the decrease in the horizontal beam axis led to only a small net change in the average beam axis, increasing by only 1.7% from 777 nm in the as-fabricated nanolattices to 790 in the irradiated nanolattices. In terms of the inner beam dimensions, the average inner beam axis measurement only increases by 1.7% upon irradiation. The apparent collapse of nanolattice beams upon irradiation is more pronounced for the thinner-walled interior beams as visualized in Figure 2 (f). The slightly elliptical shape of the beams became more elliptical upon irradiation as evidenced by the increase in the measured beam major axis and decrease in the measured beam minor axis, as shown in Table 2. Further, the  $\sim$ two-fold increase in standard deviation of these measured beam dimensions demonstrates a larger variation in inner beam dimensions upon irradiation, consistent with these shape changes.

This relative density was calculated from SolidWorks models with the specified nanolattice dimensions discussed in section 2.1 and a wall thickness of 114 nm, the average wall thickness of the as-fabricated

nanolattices formed by 240-minute sputter deposition, as shown in our previous study<sup>[21]</sup>. For this calculation the average wall thickness was chosen instead of the median wall thickness because the average is more representative of the relative density of the total nanolattice. In contrast, the median is more representative of the wall thickness relevant for the sections of nanolattice undergoing mechanical deformation.

### **Details of mechanical testing**

The absolute size of the strain burst and stress drop will depend on the details of compression test method and controls as well as the dynamics of the mechanical testing instrument used. As all nanolattices in this study were compressed utilizing an identical test method and testing instrument, a direct comparison can be made for the sizes of the strain bursts and stress drops between the as-fabricated and irradiated nanolattices, as shown in Figure 5 and discussed in section 3.3. However, the size of these strain bursts and stress drops may vary with a different mechanical testing instrument and test method; hence care should be taken in comparing the strain burst and stress drop size in this study with those in another study using different testing conditions or instrumentation.